Supporting Information

Saito et al. 10.1073/pnas.0903854106

SI Methods

Cell Lines and Isolation of Human GC Centroblasts. All B-cell lines were maintained in Iscove's modified Dulbecco's medium (IMDM) supplemented with 10% FBS, 100 IU/mL penicillin, and 100 mg/mL streptomycin (Cellgro), except for Ly10 and Ly4, which were cultured in 20% heparinized human plasma and 55 μM β-mercaptoethanol. Rat1 fibroblasts and 293T cells were maintained in Dulbecco's modified Eagle's medium (DMEM) supplemented with 10% FBS, 100 IU/mL penicillin, and 100 mg/mL streptomycin. GC centroblasts were isolated from human tonsils as described (1) and maintained in IMDM/20% FBS for 6 h, using 10 μg/mL of anti-CD40 antibody obtained from G28–5 hybridoma cells (ATCC) and 10 μg/mL of anti-IgM antibody (Southern Biotech).

DLBCL Primary Cases. Primary biopsies from 149 newly diagnosed DLBCL patients were obtained as paraffin-embedded and/or frozen material from the archives of the Departments of Pathology at Columbia University and Weill-Cornell Medical Center, after approval by the respective Institutional Review Board Committee.

Plasmids. The expression vectors encoding HA-BCL6, its deletion mutants –ΔPOZ and −ΔZF, and FLAG-Miz1 have been described (2, 3). The BCL2 wild-type and DLBCL-derived mutant reporter constructs were generated by inserting the corresponding PCR-amplified genomic region of the human BCL2 promoter (−546/+387) upstream of the luciferase gene in the pGL3b vector (Promega). The derivative reporter construct carrying mutations in the 12 BCL6 binding sites was generated by the Quick Change site-directed mutagenesis method (Stratagene).

ChIP-on-Chip Analysis. Chromatin immunoprecipitation (ChIP) was performed as previously reported (4), starting from 40×10^6 purified GC B cells and Ramos B cells and using 6 μg of anti-BCL6 antibody (N3, Santa Cruz Biotechnology) or isotype-matched polyclonal IgG (Sigma-Aldrich). All samples were preliminarily tested for BCL6 and β-actin enrichment by qPCR. BCL6-ChIP DNA and whole cell extract (input) DNA were purified, amplified, and labeled with Cy5 and Cy3, respectively. The labeled ChIP DNAs were mixed in a 1:1 ratio with their respective input DNAs and hybridized to the Human Promoter ChIP-on-chip Microarray Set (2×244 K; Agilent Technologies). Hybridization was performed for 40 h at 65 °C in a rotating oven and the slides were subsequently washed and scanned (Agilent Scanner, Agilent Technologies) following the manufacturer's indications. Analysis was performed using ChIP-on-chip significance analysis (CSA) (5), which assigns *P*-values to each probe following the conditional probability of the magnitude *M* on the amplitude *A*, where *M* is the enrichment of the immunoprecipitated channel relative to the whole-cell extract channel, and *A* is the average of the logarithm of the 2 measurements. Thus, the *P*-value ratio is the logarithm of the ratio between the significance threshold of 0.001 and the *P*-value of the individual probes, as identified by CSA.

Gene Expression Data. Gene expression profile analysis of normal B cells and primary DLBCL cases was performed using Affymetrix HG-U133Plus 2.0 arrays as part of an independent study (GEO database GSE12195). The probe sets used in Fig. 2 and Fig. 5 are Miz1 (203602_s_at), BCL2 (203685_at), and BCL6 (203140_at).

Immunohistochemistry and Immunofluorescence Analysis. DLBCL tissue microarrays (TMA) were constructed according to standard procedures and analyzed by immunohistochemistry using anti-BCL2 (clone 124) and anti-BCL6 (PG-B6p) mouse monoclonal antibodies (DAKO) and a cutoff of ≥30% positive cells. Double immunofluorescence staining was performed using anti-BCL2 (BD Bioscience; 1:2,500 dilution) and anti-BCL6 antibodies (N3, Santa Cruz Biotechnology; 1:400 dilution) and, as secondary antibodies, Cy3-conjugated donkey anti-rabbit IgG (Jackson ImmunoResearch Laboratories) and biotin-conjugated anti-mouse IgG (Vector Laboratories), followed by Streptavidin-FITC (Molecular Probes).

Analysis of BCL2 Translocations by FISH. The presence of BCL2 translocations in primary DLBCLs was assessed on TMA paraffin blocks by using a BCL2 dual color–break apart probe (Vysis), according to standard methods. Slides were evaluated for the probe signal intensity and signal to background ratio, and hybridization signals were scored on at least 500 interphase nuclei from 5 representative areas per core, on DAPI-stained slides. The background, established from normal tonsils included in each TMA, was $1.0\% \pm 2 \times 0.5$ (mean ± 2 SD), and cases were scored as positive if the rearrangement was present in at least 1 core. In total, 126 cases were considered evaluable for analysis. In 2 additional samples, BCL2-IGH rearrangements were identified by multiplex PCR amplification using genomic DNA as described (6).

qChIP Analysis. Immunoprecipitated DNA fragments were analyzed for the presence of BCL2 sequences using the primers reported in supporting information (*SI*) Table S3 and the SYBR Green PCR Master Mix (Applied Biosystems), as recommended by the manufacturer. ΔCt's were calculated for anti-BCL6 and control IgG ChIP fragments relative to their input DNA and used to calculate the ΔΔCt's. Fold changes (2-ΔΔCt) observed in BCL6 vs. control IgG samples were corrected using β-actin as a negative control. Reactions were performed in triplicate on at least 2 independent experiments.

qRT-PCR. Total mRNA extraction and cDNA synthesis were performed as reported (7), and the SYBR Green PCR Master Mix was used to measure BCL2 and BCL6 expression (see Table S3 for primers). Relative expression levels were calculated by the ΔΔCT method, using GAPDH as a reference control. All reactions were performed in triplicate on at least 2 independent experiments.

Western Blot Analysis. Total protein extracts were prepared as described (7) and analyzed using the following antibodies: anti-BCL2 (ab7973, Abcam; and 554218, BD PharMingen), anti-α-tubulin (H-235, Santa Cruz), anti-β-actin (A5441, Sigma), anti-FLAG (F-3165, Sigma), anti-HA (3F10, Roche), and anti-BCL6 (Cell Signaling Technology). The anti-Miz1 antibody was a gift from Martin Eilers.

Lentiviral Infections. Lentiviral vectors expressing BCL6 shRNAs (TRC0000013606 and TRC0000013603), Miz1/ZBTB17 shRNA (TRC0000012955 and TRC0000012956), and a control shRNA (SHC002) were purchased from Sigma, and infections were performed as reported (7). Transduced cells were selected with puromycin (0.5 μg/mL) for 2 days before collection for analysis.

Transfection of Rat1 Cells and Colony-Formation Assay. Rat1 fibroblast clones, stably expressing the PINCO-HA-BCL6 retroviral vector or control empty vector, were transfected in duplicate with BCL2 expression vectors using Lipofectamine 2000 (Invitrogen) according to the manufacturer's protocol. Stable bulk populations were obtained after selection in G418 (600 μg/mL) (Gibco). The soft agar colony formation assay was performed as previously described (8), except that IMDM supplemented with 20% non-heat-inactivated FCS was used and cells were plated in triplicate in 35 $\times$ 10-mm Petri dishes (Beckton Dickinson) at a density of 2,500, 5,000, and 10,000 cells per dish. The plates were incubated at 37 °C and colonies larger than 0.2 mm were counted after 6 days.

1. Klein U, et al. (2003) Transcriptional analysis of the B cell germinal center reaction. *Proc Natl Acad Sci USA* 100:2639–2644.
2. Phan RT, Dalla-Favera R (2004) The BCL6 proto-oncogene suppresses p53 expression in germinal-centre B cells. *Nature* 432:635–639.
3. Phan RT, Saito M, Basso K, Niu H, Dalla-Favera R (2005) BCL6 interacts with the transcription factor Miz-1 to suppress the cyclin-dependent kinase inhibitor p21 and cell cycle arrest in germinal center B cells. *Nat Immunol* 6:1054–1060.
4. Pasqualucci L, et al. (2003) Mutations of the BCL6 proto-oncogene disrupt its negative autoregulation in diffuse large B-cell lymphoma. *Blood* 101:2914–2923.
5. Margolin AA, et al. (2009) Chip-on-chip significance analysis reveals large scale binding and regulation by human transcription factor oncogenes. *Proc Natl Acad Sci USA* 106:244–249.
6. van Dongen JJ, et al. (2003) Design and standardization of PCR primers and protocols for detection of clonal immunoglobulin and T-cell receptor gene recombinations in suspect lymphoproliferations: Report of the BIOMED-2 Concerted Action BMH4-CT98–3936. *Leukemia* 17:2257–2317.
7. Saito M, et al. (2007) A signaling pathway mediating downregulation of BCL6 in germinal center B cells is blocked by BCL6 gene alterations in B cell lymphoma. *Cancer Cell* 12:280–292.
8. Hoang AT, Cohen KJ, Barrett JF, Bergstrom DA, Dang CV (1994) Participation of cyclin A in Myc-induced apoptosis. *Proc Natl Acad Sci USA* 91:6875–6879.

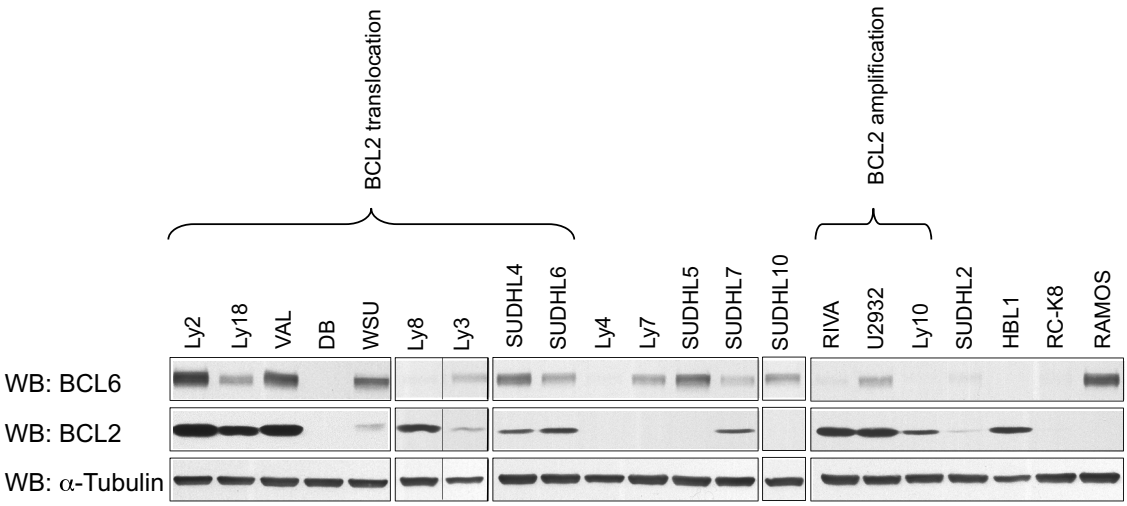

Fig. S1. Western blot analysis of BCL6, BCL2, and α-tubulin expression in DLBCL cell lines.

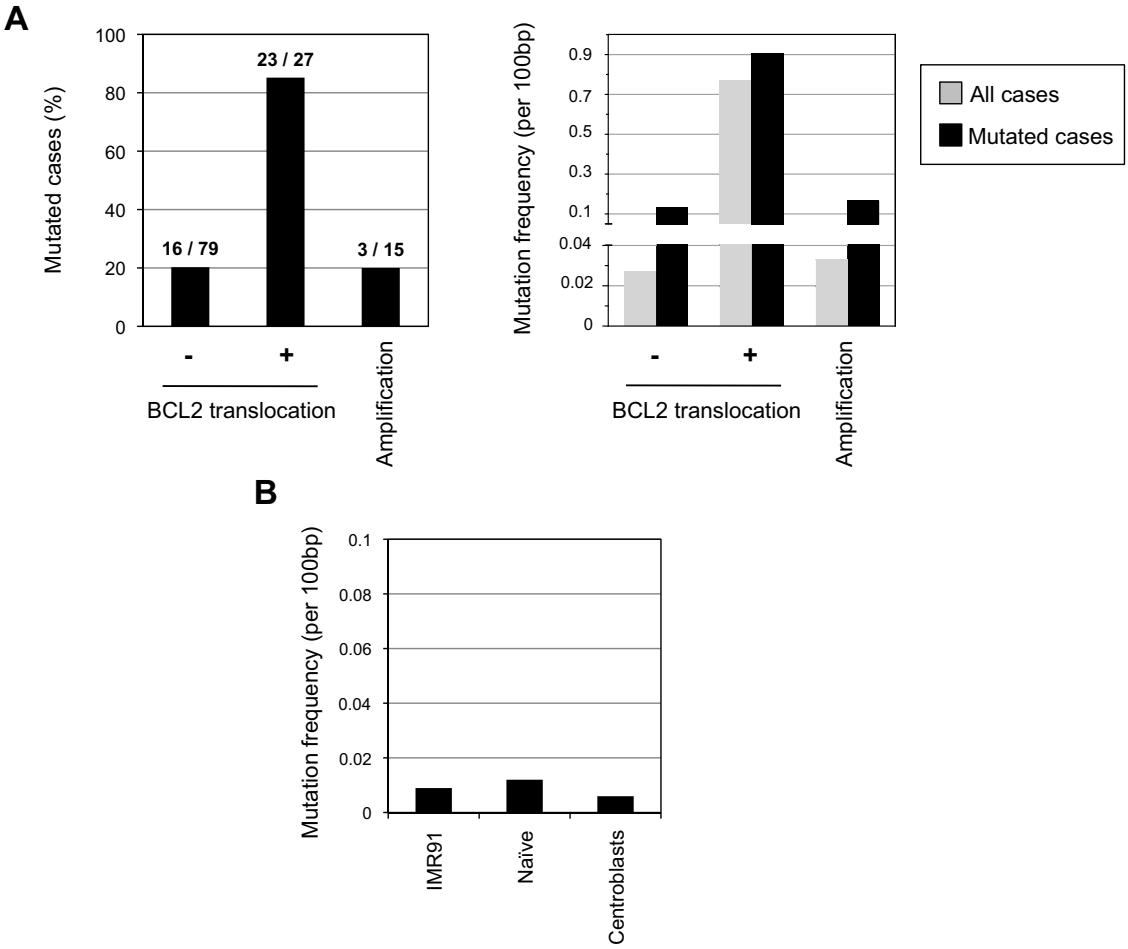

Fig. S2. BCL2 is targeted by mutations in DLBCL, but not in normal B cells. (*A*) (*Left*) Distribution of BCL2 mutated samples in DLBCL samples (cell lines and primary biopsies), with or without gross BCL2 structural alterations. The total number of mutated samples over total sequenced is shown at the top. (*Right*) BCL2 mutation frequencies in the same DLBCL groups, as obtained by direct sequencing. Frequencies are calculated in the 2-kb region (−400 to +1600) that was found mutated in >95% of the affected cases, considering 2 alleles per sample in all cases sequenced (shaded bars) or in mutated cases only (solid bars). (*B*) BCL2 mutation frequencies in normal B cells (naive and centroblasts) (region +35 to +700). The fibroblast cell line IMR91, which does not undergo SHM, was included as control for the polymerase error rate. Data were obtained from sequencing analysis of cloned PCR products ($n = 48$ each) and, as such, cannot be compared to the mutation frequencies measured in *A* by direct sequencing.

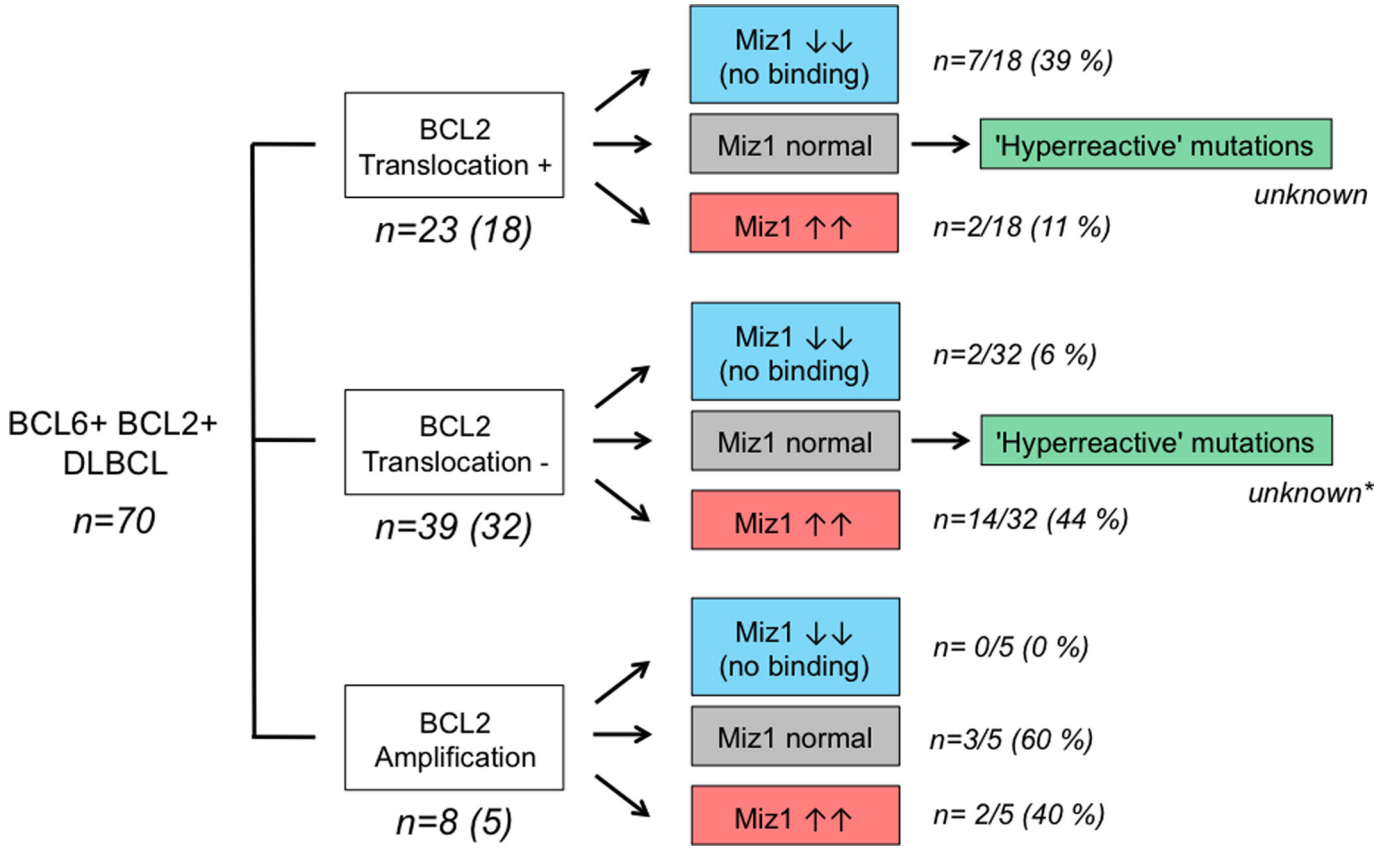

Fig. S3. Model for the mechanisms leading to pathologic coexpression of BCL6 and BCL2 in DLBCL. The total number of cases in each DLBCL group, including cell lines and primary biopsies, is indicated (in parentheses, number of samples with available Miz1 expression data). (*) Note that the only mutated sample in this group, which includes mostly unmutated cases, displayed abnormal response to Miz-1-induced activation.

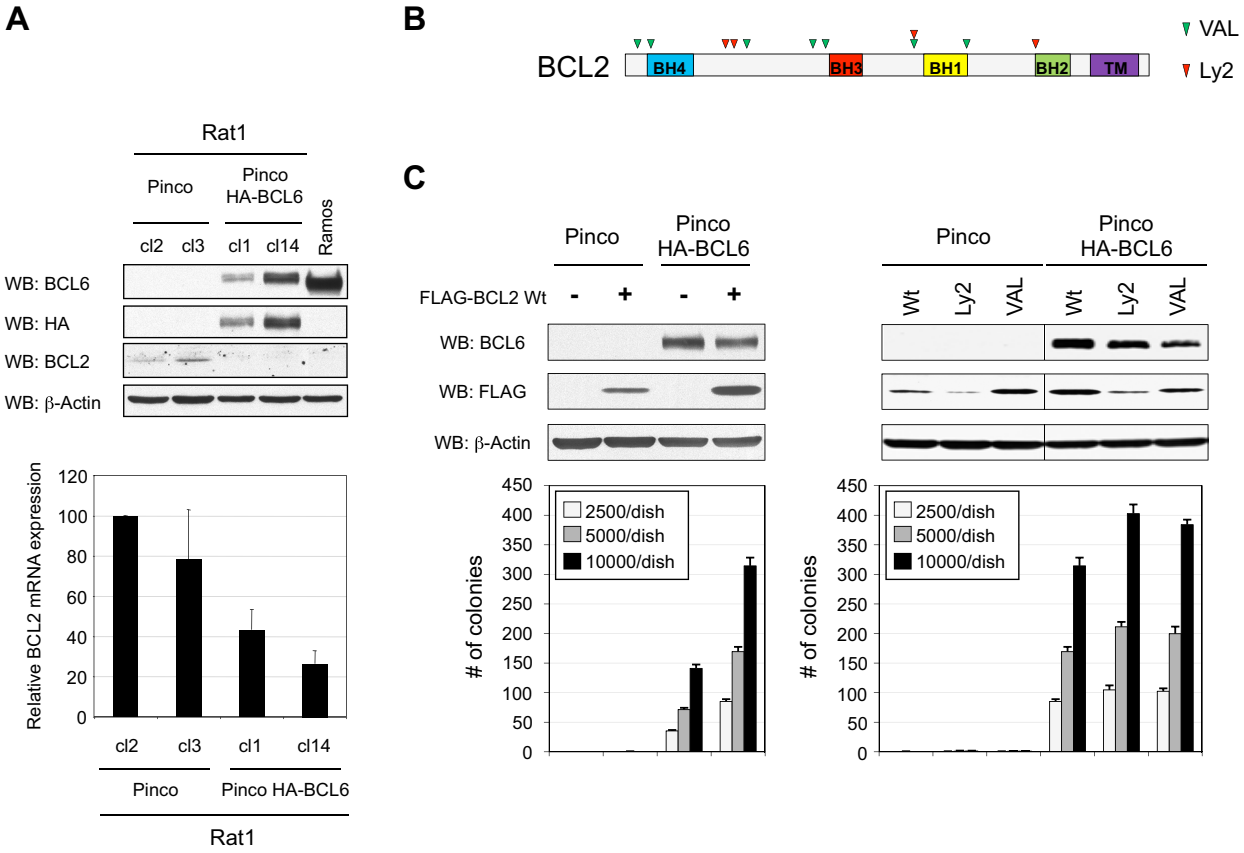

Fig. S4. Synergistic BCL6 and BCL2 transformation ability in Rat1 cells. (*A*) Western blot analysis of exogenous BCL6 and endogenous BCL2 expression in Rat1 clones stably transduced with Pinco-HA-BCL6 or empty vector. (*Upper*) The Ramos cell line is used as a control for endogenous BCL6 protein levels. (*Lower*) BCL2 mRNA expression in the same clones was measured by qRT-PCR. (*B*) Schematic representation of the BCL2 protein, with its relevant functional motifs: BH, BCL2 homology motif; TM, transmembrane motif. Color-coded symbols depict missense mutations observed in the BCL2 alleles from 2 cell lines (Ly2, VAL) that were tested in soft agar/colony formation assays. (*C*) (*Upper Left*) Western blot analysis of exogenous BCL6 and BCL2 expression in Rat1 cells stably expressing HA-BCL6 and wild-type FLAG-BCL2 (or control empty vector). (*Lower Left*) The number of colonies larger than 0.2 mm, obtained from the same cell populations in soft agar/colony formation assays after 6 days incubation at 37 °C (3 seeding densities, in triplicate). (*Lower Right*) Transforming activity of two DLBCL-derived mutant BCL2 alleles, as compared to wild type, in the same assay. (*Upper Right*) Western blot analysis of exogenous BCL6 and BCL2 (FLAG) expression in the same Rat1 cell populations.

Other Supporting Information Files

Table S1
Table S2
Table S3